HIGH RESOLUTION EXPERIMENTAL MEASUREMENTS OF RICHTMYER-MESHKOV TURBULENCE IN FLUID LAYERS AFTER RESHOCK USING SIMULTANEOUS PIV-PLIF

B. J. Balakumar, K. P. Prestridge, G. Orlicz, S. Balasubramanian, C. Tomkins[1]

[1]*Mail Stop H803, Los Alamos National Laboratory, Los Alamos, NM 87545*

Abstract. True ensemble-averaged density self-correlation and Reynolds stress turbulence statistics in a Richtmyer-Meshkov unstable fluid layer after reshock are measured for the first time using simultaneous Particle-Image Velocimetry (PIV)-Planar Laser-Induced Fluorescence (PLIF) diagnostic. These high-quality experiments with advanced diagnostics provide important insights into the physics of RM turbulence that cannot be obtained using simple shadowgraphy or Schlieren diagnostics. The double peaked nature of the density self-correlation and the asymmetric character of the Reynolds stress distributions are discussed. Error estimates and convergence rates for several turbulence quantities are also provided.

Keywords: Richtmyer Meshkov, Turbulence, Instability, PIV, PLIF, Mixing, density self correlation.
PACS: 47.20.-k, 47.40.Nm, 47.32.-y.

INTRODUCTION

Recent advances in the application of PIV-PLIF diagnostics to RM flows [2] promise to provide a more detailed and far more incisive picture of the physics of RM mixing than the data from simple optical, hot-wire or laser-Doppler diagnostics available thus far [5,6]. The new diagnostics allow the direct measurement (and therefore, the modeling) of several turbulence quantities for the first time. For example, the density self-correlation parameter ($b = -\langle \rho'(1/\rho)' \rangle$), which is a measure of the mixing state, appears unclosed in the production term of the mass flux equation and requires a model. This term influences the mixing directly (in conjunction with the density gradient) as evidenced by the production term in the evolution equation for ***b*** (Ref: LANL's BHR model). In this paper, we will discuss selected results concerning the measurement of density self-correlation and one component of the generalized Reynolds stress ($R_{12} = \langle \rho u'' v'' \rangle$) using simultaneous PIV-PLIF diagnostics. We will also discuss the errors associated with such measurements along with the convergence rate estimates for the turbulence data.

EXPERIMENTAL PROCEDURE

The data presented in this paper were acquired at the Los Alamos National Laboratory's horizontal shock tube facility. Equipped with state of the art PIV and PLIF diagnostics, and using a novel method to create extremely stable, membrane-free initial conditions, simultaneous density and velocity measurements were obtained in an evolving RM unstable fluid layer after first shock and after reshock. Detailed descriptions of the experimental facility and diagnostics are provided elsewhere [2].

Experimental uncertainties: PIV

The primary source of error from typical PIV measurements is the random error introduced by the sub-pixel estimators. This error has been estimated to be $0.1\,d_\tau$, where d_τ is the diameter of the particles as imaged through the camera. In the

present case, d_τ is about 1 pixel. Therefore, for a typical pixel displacement of 5 pixels between the cross-correlation image pairs, the error in each velocity vector measurement is about 2%.

Perspective error in the present experiments arises from the non-orthogonality of the camera axis and the laser light-sheet. These errors are corrected by imaging a calibration target and performing a projective transform on the images. The projective transform can correct for location errors to within $\pm 27.3\,\mu m$. The perspective correction is also used to superimpose the PIV vector fields on the PLIF images.

Uncertainty due to refractive index variations in the mixing zone due to temperature, concentration and pressure fields in the flow is less than 0.0012 for viewing angles of less than 30°, as calculated using Gladstone-Dale equations [2].

Experimental uncertainties: PLIF

Errors in PLIF measurements are primarily attributable to the calibration process, the presence of inhomogeneities in the laser beam, and to the response variations between pixels in the CCD camera (flat-field). The present Quantitative-PLIF (QPLIF) measurements were calibrated prior to data acquisition by flowing SF_6 mixed with acetone through a nozzle. The detailed calibration procedure is provided in Balakumar et al. [2].

Errors could be introduced in the QPLIF measurements of density by the variability of the light sheet (between shots and within a single shot). Often, the light-sheet variability within a single shot is corrected by measuring the average spanwise profile of the light-sheet during the calibration phase. This profile is obtained either by direct measurement or by seeding the test section with a uniform concentration of acetone vapor [7]. The shot-to-shot variability in the output power of the laser is corrected by direct measurement using fast-response power meters. In the present case, the standard deviation of the laser output is measured to be $\pm 5\%$. The validity of this procedure depends on the stability of the laser resonator, however.

The lack of spanwise similarity of beam profiles after correcting for the total power was investigated by measuring the profiles of five consecutive PLIF pulses using a beam profiler (Ophir Spiricon SP03U). The laser was pulsed continuously at 5Hz for more than 5 minutes before the measurements were obtained. The sensor was located near the center of the laser light sheet in the test section to capture a region 4.6mm in width. Figure 1 shows the raw beam profiles measured by the profiler. The power variations and spanwise variations are clear. Upon normalizing each of the profiles with the total energy (by integrating the signal in the spanwise direction), most of the signal appears to collapse into a single (mean) profile. However, away from the center of the beam, in the regions marked by arrows, significant fluctuations are observed in the beam profiles and the similarity of the beam profile breaks down.

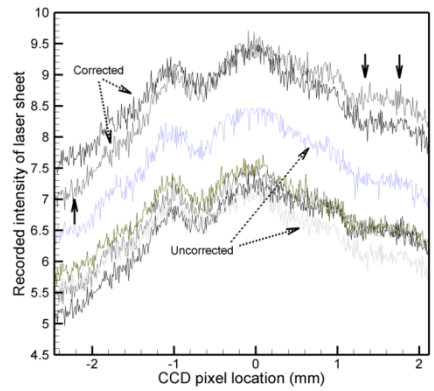

FIGURE 1. Laser profiles before and after correction for gross-intensity variations. The lack of similarity near the edges of the corrected beams is an indicator of the unstable laser resonator.

Thus, the measurement of quantitative turbulent density fields using QPLIF requires the simultaneous use of a CCD-based beam profiler for each instantaneous realization to compensate for beam profile variations in Nd:YAG lasers. Other researchers have found that stable resonators in some XeF excimer lasers result in excellent repeatability [4].

Convergence of turbulence statistics

In canonical turbulence, care must be taken to ensure the independence of each instantaneous measurement in order to invoke ergodicity. However, this independence is automatically ensured (by definition) in the measurement of true ensemble statistics. In this special case, when the instantaneous measurements are independent of one another, the standard deviation of the mean

value estimate and the unbiased variance estimator are calculated using [3]:

$$\sigma_{\hat{x}} = \left(\frac{\sigma_{TI}^2 + \sigma_M^2}{N} \right)^{1/2} \quad \& \quad \sigma_{\hat{\sigma}_x^2} = 2\left(\frac{\sigma_{TI}^4 + \sigma_M^4}{N-1} \right)^{1/2} \qquad (1)$$

where σ_{TI} is the RMS value of the turbulence fluctuations of the variable and σ_M is the RMS of the measurement error.

Therefore, a two-fold increase in the accuracy of the estimated mean and turbulence statistics would require a four-fold increase in the number of samples. This slow decay of the error, for the streamwise velocity fluctuations in the turbulent flow after reshock, is shown in Fig 2 for values of σ_{TI} = 4 m/s and σ_M = 0.3 m/s. The value of the turbulence intensity used here is obtained from whole-field histograms of the streamwise velocity fluctuations [2] and the measurement error was assumed to be the consequence of random sub-pixel estimation errors [1]. Thus, the estimation of the streamwise velocity variance to accuracy greater than 20% would require more than 1500 instantaneous realizations. For these experiments, each PIV realization is capable of capturing the velocity field within 5 adjacent wavelengths of the initial condition. Assuming independent evolution between the wavelengths, about 300 runs of the experiment are required to obtain convergent streamwise velocity fluctuation statistics. For such an ensemble, the standard deviation of the mean velocity is less than 0.1m/s.

The standard deviation of the estimate of the density self-correlation can be derived to be

$$\sigma_{\hat{b}} = \frac{\sigma_\rho}{\langle \rho \rangle \sqrt{N}} \sqrt{\begin{array}{l} \langle \rho \rangle^4 \left\langle \frac{1}{\rho^4} \right\rangle + (1+b)^2 \\ -2(1+b)\langle \rho \rangle^2 \left\langle \frac{1}{\rho^2} \right\rangle \end{array}} \qquad (2)$$

Once again, the slow rate of convergence of this statistic with the number of realizations is evident.

Experience has shown that spanwise-averaged 1-D statistics are often useful for the validation of computations. Since each PIV velocity field in the present experiments provides about 60 velocity vectors in the spanwise direction, a dramatic reduction in the errors can be expected for even nominal ensemble sizes. However, one must remember that the increase in N is associated with a corresponding increase in σ_{TI} as the turbulence fluctuations are now spanwise averages of single-point statistics. Further Eqns. 1-2 are no longer valid as the realizations that constitute the ensemble are no longer independent of one another. Therefore, the new error estimates would include spatial correlations in addition to the instantaneous turbulence quantities [1].

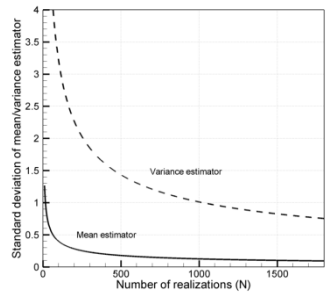

FIGURE 2. Convergence rate estimates of some turbulence quantities.

RESULTS AND DISCUSSION

The turbulence statistics presented in this paper have been calculated from 9 closely repeatable instantaneous realizations selected from a total of 35 runs of the experiment to satisfy strict criteria for repeatability [2]. All the data were obtained from varicose initial conditions created by the diffusion of the heavy gas from a row of 3.0mm cylindrical nozzles separated by 3.6mm.

The evolution of the density self-correlation parameter (*b*) at 4 times after reshock is shown in Fig. 3. These measurements show the streamwise variation of the *b* fields after spanwise averaging the ensemble. The double peaked structure of *b* is evident at all times. The peaks coincide with the edges of the turbulent mixing structure while the trough occurs near the center of the structure (where the most amount of mixing has occurred and driven the flow to near homogeneity). Near the edges, the entrainment of the surrounding air would create large density fluctuations contributing to the observed peaks. At the earliest time observed (t=665 μs or 65 μs after reshock), the dissociation of the ordered flow into the smaller scales is incomplete resulting in a *b* profile that is different from those of the later times. Once the

disintegration of the flow into the smaller scale structures is complete, the evolution of the *b* profiles slows down considerably and remains roughly similar for the next 150 μs .

Fig. 4 shows contours of R_{12} calculated at t=115 μs after reshock. While whole-field histograms of R_{12} follow a symmetric distribution with equal contributions of positive and negative values [2], contour spatial maps of R_{12} clearly show a streamwise asymmetry. Large fluctuations preferentially occur upstream of the centerline while moderate fluctuations dominate the downstream direction. Thus, despite the similar Mach numbers of the shock and reshock wave, it appears that the flow contains inhomogeneities in the turbulence statistics. This is a clear demonstration of the value of simultaneous PIV-PLIF diagnostics over conventional PLIF / Schlieren / Shadowgraph diagnostics to provide illuminating insights into RM turbulence.

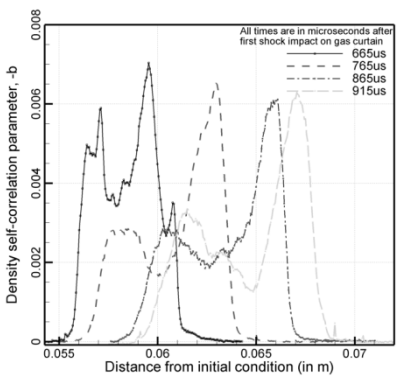

Figure 3. The density self-correlation parameter, "b", for four times after reshock.

CONCLUSIONS

Estimates of two important turbulence quantities, namely, the density self-correlation parameter, *b*, and the generalized Reynolds stress tensor, R_{12}, have been experimentally obtained in Richtmyer-Meshkov unstable fluid layers for the first time. Detailed error estimates of the various components of the PIV/PLIF diagnostics have been provided along with statistical convergence rates for some of the turbulence quantities. Direct measurements of the laser beam profile used for QPLIF measurements were used to demonstrate the importance of recording the instantaneous profile variations for every shot in addition to the total pulse energies for lasers with unstable resonators.

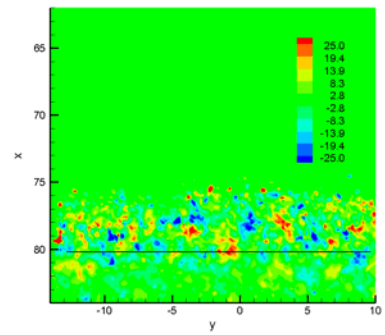

FIGURE 4. Contour plot of the general Reynolds stress, R_{12}, from simultaneous PIV/PLIF measurements.

ACKNOWLEDGEMENTS

This work was supported by the Department of Energy under Contract No. DE-AC52-06NA25396.

REFERENCES

1. Adrian, R. J., and Westerweel, J., "Particle-Image Velocimetry", Cambridge University Press, New York, 2009 (in press).
2. Balakumar, B. J. et. al., "Simultaneous Particle-Image Velocimetry-Planar Laser-Induced Fluorescence Measurements of Richtmyer-Meshkov Instability Growth in a Gas Curtain with and without Reshock", Phys. Fluids 20, 124103, 2008.
3. Bevington, P. R., "Data Reduction and Error Analysis for the Physical Sciences", McGraw-Hill, New York, 1969.
4. Cruyningen, I., "Quantitative Imaging of Turbulent Gaseous Jets using Planar Laser-Induced Fluorescence" PhD Thesis, Stanford University, 1990.
5. Jourdan, G. et al., "Hot-wire method for measurements of turbulent mixing introduced by Richtmyer-Meshkov instability in shock tube", 11(3), 189-197, Shock Waves, 2001.
6. Poggi, F. et. al., "Velocity Measurements in Turbulent Gaseous Mixtures Induced by Richtmyer-Meshkov Instability", Phys. Fluids, 10(11), 2698-2700, 1998.
7. Tomkins C. et. al. "An Experimental Investigation of Mixing Mechanisms in Shock-accelerated Flow", J. Fluid Mech., 611, 131-150, 2008.